Editor's Choice

Responses to iron limitation are impacted by light quality and regulated by RcaE in the chromatically acclimating cyanobacterium *Fremyella diplosiphon*

Bagmi Pattanaik,[1]† Andrea W. U. Busch,[1] Pingsha Hu,[1]‡ Jin Chen[1] and Beronda L. Montgomery[1,2]

Correspondence
Beronda L. Montgomery
montg133@msu.edu

[1]Department of Energy – Plant Research Laboratory, Michigan State University, East Lansing, MI 48824, USA

[2]Department of Biochemistry and Molecular Biology, Michigan State University, East Lansing, MI 48824, USA

Photosynthetic organisms adapt to environmental fluctuations of light and nutrient availability. Iron is critical for photosynthetic organismal growth, as many cellular processes depend upon iron cofactors. Whereas low iron levels can have deleterious effects, excess iron can lead to damage, as iron is a reactive metal that can result in the production of damaging radicals. Therefore, organisms regulate cellular iron levels to maintain optimal iron homeostasis. In particular, iron is an essential factor for the function of photosystems associated with photosynthetic light-harvesting complexes. Photosynthetic organisms, including cyanobacteria, generally respond to iron deficiency by reduced growth, degradation of non-essential proteins and in some cases alterations of cellular morphology. In response to fluctuations in ambient light quality, the cyanobacterium *Fremyella diplosiphon* undergoes complementary chromatic adaptation (CCA). During CCA, phycobiliprotein composition of light-harvesting antennae is altered in response to green light (GL) and red light (RL) for efficient utilization of light energy for photosynthesis. We observed light-regulated responses to iron limitation in *F. diplosiphon*. RL-grown cells exhibited significant reductions in growth and pigment levels, and alterations in iron-associated proteins, which impact the accumulation of reactive oxygen species under iron-limiting conditions, whereas GL-grown cells exhibited partial resistance to iron limitation. We investigated the roles of known CCA regulators RcaE, RcaF and RcaC in this light-dependent iron-acclimation response. Through comparative analyses of wild-type and CCA mutant strains, we determined that photoreceptor RcaE has a central role in light-induced oxidative stress associated with iron limitation, and impacts light-regulated iron-acclimation responses, physiologically and morphologically.

INTRODUCTION

Iron is a key element with functional as well as structural importance and is required for the growth of organisms from microbes (Hantke, 2001) to eukaryotes (Castagna *et al.*, 2009; Connolly & Guerinot, 2002; de Silva *et al.*, 1996; Walker & Connolly, 2008). Iron is required for a number of critical cellular functions, including haem and chromophore synthesis, haem-dependent oxygen transport, redox reactions, iron-dependent enzymic reactions, ribonucleotide synthesis and photosynthesis (Straus, 1994); thus, the regulation of iron availability is central to optimal growth and productivity. Iron is essential for the activity of photosystems functionally linked to photosynthetic light-harvesting complexes in many organisms capable of oxygenic photosynthesis, including cyanobacteria. Iron is a component of iron–sulfur (Fe–S) clusters, haem-containing cytochromes and nonheme iron that serve as cofactors in photosynthetic protein complexes (reviewed by Shcolnick & Keren, 2006). In cyanobacteria, the functional photosynthetic apparatus requires ~ 22–23 iron atoms for photosysytem I (PS I) and PS II, the cytochrome b6/f complex and ferredoxin (reviewed by

Abbreviations: AP, allophycocyanin; CCA, complementary chromatic adaptation; chl*a*, chlorophyll *a*; DCFH-DA, 2′,7′-dichlorodihydrofluorescein diacetate; DIC, differential interference contrast; FeSOD, iron-containing superoxide dismutase; GL, green light; ICP-OES, inductively coupled plasma optical emission spectrometry; PBP, phycobiliprotein; PBS, phycobilisome; PC, phycocyanin; PE, phycoerythrin; RL, red light; ROS, reactive oxygen species; SOD, superoxide dismutase.

Ferreira & Straus, 1994). Although iron is not a component of the photosynthetic phycobilisomes (PBSs) of cyanobacteria, it is critical for PBS synthesis and function: chromophores of phycobiliproteins (PBPs) are derived from iron-containing haem (Terry *et al.*, 2002) and their synthesis requires ferrodoxin-dependent reductases (reviewed by Dammeyer & Frankenberg-Dinkel, 2008). Thus, the availability of iron is crucial in determining the regulation and function of photosynthetic growth in these organisms. Although iron is an essential metal in most biological systems, in excess it can cause deleterious effects, as it is a highly reactive metal that can result in the generation of damaging radicals *in vivo* (Shcolnick & Keren, 2006). The bioavailability of iron is limited in the environment because it is complexed in iron oxides. These features – i.e. the essential nature of iron in biological organisms, the potential toxicity of iron at high levels and the limited availability of this element in natural environments – necessitate finely tuned regulatory mechanisms to maintain organismal iron homeostasis.

Because of the high requirement of iron in photosynthesis, iron deficiency generally limits the growth of photosynthetic organisms. Iron has been shown to be limiting in both marine (Behrenfeld *et al.*, 1996) and freshwater aquatic environments (Sterner *et al.*, 2004; Twiss *et al.*, 2000). In addition to lower growth rates, iron limitation also modulates other physiological processes and the morphology of some cyanobacteria (for a review see Montgomery & Pattanaik, 2010). Iron limitation has been shown to result in low levels of accumulation of photosynthetic PBPs, chlorophyll *a* (chl*a*) and carotenoids in several cyanobacterial systems, including two strains of *Microcystis* (Xing *et al.*, 2007), *Anaebaena* sp. PCC 7120 (Narayan *et al.*, 2011), *Synechococcus* sp. PCC 7942 (Fraser *et al.*, 2013; Sandström *et al.*, 2002) and *Synechocystis* sp. PCC 6803 (Fraser *et al.*, 2013). Under iron-limited growth conditions, cyanobacteria such as *Trichodesmium* IMS101 maintain overall levels of the photosynthetic apparatus (i.e. PBSs), but modify PBS protein composition (Küpper *et al.*, 2008). The impact of iron on growth may be a direct consequence of the described effects of iron deficiency on the levels of photosynthetic proteins and the related reduction in photosynthetic capacity in cyanobacteria.

Iron-limitation stress results in an elevated level of reactive oxygen species (ROS) in part because several ROS-detoxifying enzymes – such as catalases, peroxidases or some superoxide dismutases (SODs) – require iron as a cofactor (Michel & Pistorius, 2004). Oxidative stress negatively impacts photosystem function (Bhaya *et al.*, 2000). Latifi *et al.* (2005) confirmed that iron-limited growth is associated with oxidative stress. These authors reported a 10-fold increase in the amount of ROS under iron-limited growth in *Anabaena* sp. strain PCC 7120 (Latifi *et al.*, 2005).

Iron-limited cyanobacteria can exhibit altered cellular morphology, and such morphological differences associated with iron limitation are species specific. Iron limitation has been associated with reduced cell length in the cyanobacteria *Anacystis nidulans* R2 (Sherman & Sherman, 1983)

and *Synechococcus elongatus* (Benešová *et al.*, 2000). By contrast, in *Trichodesmium* IMS101 no effect on cell length was reported, but fragmented and shorter filaments were observed under iron-limited conditions (Küpper *et al.*, 2008). In *Fremyella diplosiphon*, we reported a light-dependent cellular morphology change with enlargement and vacuolation in cells under iron-limited conditions (Pattanaik & Montgomery, 2010).

F. diplosiphon is a model cyanobacterium classically used for the study of light-dependent regulation of photosynthetic efficiency. This organism displays light quality-regulated photosynthetic pigment accumulation through a well-characterized molecular process historically known as complementary chromatic adaptation (CCA; Tandeau de Marsac, 1977). CCA is regulated by the photoreceptor RcaE and its downstream response regulators RcaF and RcaC, particularly in response to green light (GL) and red light (RL) (reviewed by Gutu & Kehoe, 2012; Kehoe & Gutu, 2006). Upon mutation of the genes encoding these proteins, the colour phenotype (Kehoe & Grossman, 1996, 1997), as well as the morphology of cells, is altered (Bordowitz & Montgomery, 2008; Bordowitz *et al.*, 2010). During CCA in *F. diplosiphon*, genes whose expression levels were regulated by light were implicated in iron-related processes (Stowe-Evans *et al.*, 2004). Furthermore, we previously observed that iron limitation under RL results in a stronger decrease in growth than iron limitation under GL in *F. diplosiphon* (Pattanaik & Montgomery, 2010). Here, we report the investigation of the impact of iron limitation on growth, development and oxidative stress levels, as well as the role of known CCA regulators on wavelength-dependent photoacclimation to iron limitation. We describe genotype-specific physiological and morphological responses under iron-limited conditions during the process of CCA. Physiological, morphological and transcriptomics analyses indicate that the photosensor RcaE plays a central role in the regulation of light-dependent responses to iron limitation in *F. diplosiphon*.

METHODS

Cyanobacteria strains and culture conditions. In this study, we used *F. diplosiphon* strain SF33, a wild-type pigmentation strain that exhibits shortened filaments (Cobley *et al.*, 1993), the photoreceptor mutant Δ*rcaE* (FdBk14; Kehoe & Grossman, 1996) and response regulator mutants Δ*rcaF* (FdR101; Bordowitz & Montgomery, 2008) and Δ*rcaC* (FdR102; Bordowitz & Montgomery, 2008). All mutant strains were derived in the SF33 background. The pigmentation and morphology of the *F. diplosiphon* strains used in this study when grown in replete media have been described in detail elsewhere (Bordowitz & Montgomery, 2008; Bordowitz *et al.*, 2010; Kehoe & Grossman, 1996). Cultures were grown at 28 °C with shaking under GL or RL as described previously (Bordowitz & Montgomery, 2008). GL (λmax 530 nm; Geneva Scientific) and RL (λmax 660 nm, 2506RD; LED Wholesalers) sources were identical to those detailed previously (Bordowitz & Montgomery, 2008). A Li-Cor light meter (model LI-250) connected to a Li-Cor quantum sensor (model LI-190SA) was used to measure light intensities.

Iron-replete (BG-11) and iron-limited media (BG-11₋Fe) were prepared as described previously (Pattanaik & Montgomery, 2010). BG-11 and

BG-11$_{-Fe}$ media contained 20 mM HEPES at pH 8.0. Strains maintained on agar plates were inoculated in liquid BG-11 medium and grown under GL or RL conditions for 7 to 10 days, or for 15 days for iron-containing SOD (FeSOD) assays. All glassware used in the iron-limited experiments was washed three times with water treated with Chelex-100 resin (Bio-Rad) to reduce traces of iron (Sherman & Sherman, 1983). Prior to final dilution, cells that were grown in iron-deficient growth experiments were washed three times with BG-11$_{-Fe}$ medium. Cultures were diluted to an optical density at 750 nm of ~0.1 in BG-11 or BG-11$_{-Fe}$ to initiate experiments. For iron-recovery experiments, cells grown in BG-11 or BG-11$_{-Fe}$ media for 15 days were washed three times in BG-11 before inoculation in BG-11 medium.

Cell-density measurements. Culture growth was measured as optical density, i.e. OD$_{750}$, using a SpectraMax M2 microplate reader (Molecular Devices) at 3-day intervals up to 15 days after the cells had been inoculated into BG-11 or BG-11$_{-Fe}$ medium. Three independent biological replicates were carried out in each light condition.

Preparation of samples for iron-content analysis by inductively coupled plasma optical emission spectrometry (ICP-OES). Cells were grown in 20 ml BG-11 or BG-11$_{-Fe}$ medium in RL or GL as described above for 15 days. Cells were harvested at ~ 5000 g at 4 °C for 10 min. Cell pellets were washed twice with 10 ml (10 mM) MES buffer with 10 mM EDTA at pH 5. Washed pellets were dried in a vacuum manifold with heat. A 2 ml aliquot of nitric acid (Trace metal grade, 67–60 %; Fisher Scientific) was added to each dried pellet and pellets were extracted at 100 °C for 4 h. Samples were diluted with Chelex-treated water to ~5 % nitric acid. Iron content was determined by ICP-OES at the University of Georgia Center for Applied Isotope Studies (Athens, GA, USA).

Quantification of chl$a$ and PBPs. Cells grown in BG-11 or BG-11$_{-Fe}$ medium in either RL or GL were adjusted to an OD$_{750}$ of ~0.1 on days 0 and 15 before extraction of pigments. Cell pellets were frozen in liquid nitrogen and stored at −80 °C until the extraction of pigments. chl$a$ and PBPs were extracted, analysed and quantified as described elsewhere (Bordowitz & Montgomery, 2008; Kahn et al., 1997; Tandeau de Marsac & Houmard, 1988). Averages ($\pm$SD) were calculated for data obtained from three independent experiments.

Confocal microscopy-based analysis of cellular morphology. Slide preparation and imaging parameters were followed as described previously (Bordowitz & Montgomery, 2008, 2010). Cellular morphology from each strain under both light conditions was analysed after 15 days of growth in BG-11 or BG-11$_{-Fe}$ medium by confocal microscopy. Differential interference contrast (DIC) and autofluorescence images were acquired using an inverted Axiovert 200 Zeiss LSM 510 Meta confocal laser scanning microscope (Carl Zeiss MicroImaging) as previously described (Bordowitz & Montgomery, 2008, 2010) and images processed using the LSM FCS Zeiss 510 Meta AIM imaging software.

Detection of ROS. We used 2′,7′-dichlorodihydrofluorescein diacetate (DCFH-DA; Calbiochem, EMD Biosciences) to detect the production of ROS as previously detailed (Singh & Montgomery, 2012) from WT and all the mutants grown in iron-replete or iron-limited conditions under GL or RL for 15 days. DCFH-DA (5 μM final concentration) was added to 1 ml (OD$_{750}$ ~0.1) culture. Cultures with the dye were incubated on a shaker at room temperature in the dark for 1 h (He & Häder, 2002; Rastogi et al., 2010). DCFH-DA is a nonpolar dye that is converted to the polar derivative DCFH by cellular esterases. DCFH is nonfluorescent, but is converted to highly fluorescent DCF when oxidized by intracellular ROS or other peroxides. DCF has an excitation wavelength of 485 nm and an emission peak at 520 nm. DCF fluorescence was measured in the dark using a SpectraMax M2 microplate reader (Molecular Devices).

Fluorescence was also measured for the BG-11 medium, with or without iron, mixed with dye as a negative control.

RNA-Seq differential expression analysis. RNA was extracted as previously detailed (Singh & Montgomery, 2013). Construction of cDNA libraries and Illumina sequencing was conducted at the Research Technology Support Facility at Michigan State University (East Lansing, MI, USA). An Illumina Genome Analyser II was used to generate 35 nt single-end reads. For each treatment, RNA-Seq reads were aligned to a F. diplosiphon draft genome sequence (David Kehoe, Indiana University, Bloomington, IN, USA, personal communication) using Bowtie (Langmead et al., 2009). We considered each continuous genome region covered by at least 10 reads as potential transcript fragments. All transcript fragments retrieved from each treatment were used for annotation. We predicted ORFs using prokaryote gene prediction software Glimmer3 (Delcher et al., 2007), which were compared to the generated transcripts to verify the ORFs predicted by the software. After accounting for ORFs that were fully included in the transcript fragments and using transcript fragments that overlapped with Glimmer ORFs or those that did not, which we considered as missed by Glimmer, we retrieved a total of 6828 ORFs. These ORFs were compared against Anabaena variabilis ATCC 29413 annotated proteins using BLASTX with a cut-off e value of 0.0001. For each biological sample, gene expression levels were estimated by counting reads that mapped to the annotated ORFs using HTSeq (http://www-huber.embl.de/users/anders/HTSeq/doc/overview.html). Based on the read counts, differential expression analysis between two treatments was calculated by DESeq (Anders & Huber, 2010). We assessed predicted annotations to identify proteins associated with responses to iron limitation, including catalases, peroxidases and SODs (Michel & Pistorius, 2004).

Detection of SOD by non-denaturing PAGE and immunoblot analyses. For detection of SOD, protein extracts obtained from non-denaturing lysis of F. diplosiphon cells using CelLytic B (Sigma), which was supplemented with lysozyme and benzonase as per the manufacturer's instructions, were separated by non-denaturing PAGE using a method modified from that described elsewhere (Beauchamp & Fridovich, 1971). Gels were prepared with 0.375 M Tris/HCl, pH 8.8, and 30 %/0.8 % (w/v) acrylamide/bis-acrylamide solution to a concentration of 10 % acrylamide in the separating gel and 4 % in the stacking gel with 0.1 % TEMED (N, N, N', N'-tetramethylethylenediamine) and 0.1 % (w/v) ammonium persulfate. A total of 60 μg proteins were loaded in each lane. After electrophoresis, gels were soaked in 2.5 mM nitro blue tetrazolium in P-buffer (20 mM NaH$_2$PO$_4$, 20 mM Na$_2$HPO$_4$ and 500 mM NaCl) at pH 7.8 for 30 min. Gels were then soaked in phosphate buffer containing 28 mM TEMED and 28 μM flavin and soaked for 20 min in darkness. Gels were then rinsed twice with P-buffer and thereafter exposed to fluorescent light at an intensity of 20 μmol m^{-2} s^{-1} for 15 to 20 min to initiate the photochemical reaction. Regions with SOD activity were indicated by white bands on a darker blue background. All procedures were carried out at room temperature.

For immunodetection of FeSOD, the separated proteins were blotted using a semi-dry system (Bio-Rad) for 20 min at 20 V and constant 1 A on PVDF membrane. The membrane was incubated for 1 h in blocking solution [3 % BSA, 0.5 % Tween 20 in Tris-buffered saline (TBS) buffer containing 20 mM Tris and 150 mM NaCl at pH 7.5] with shaking. The primary anti-FeSOD antibody (Agrisera) was added at 1 : 3000 dilution in blocking solution and incubated for 16 h at 4 °C with shaking. The membrane was washed four times with 10 ml TBS buffer containing 0.1 % Tween 20 for 10 min before addition of anti-rabbit secondary antibody conjugated with horseradish peroxidase (Thermo Scientific Pierce) at 1 : 10000 dilution in wash buffer. After incubation for 1 h at room temperature the wash was repeated with two additional washing steps in TBS buffer for 5 min each. FeSOD was visualized with the WesternBright ECL Western blotting detection kit (Advansta) on a VersaDoc MP 4000 imager (Bio-Rad).

RESULTS

Iron limitation impacts the growth rate of *F. diplosiphon*

F. diplosiphon exhibits decreased growth in iron-limited medium under either RL or GL, as evidenced in growth curves by a slower rate of growth, which was measured as OD_{750} at 3 day intervals, relative to cells grown in iron-replete medium (Fig. 1a, b; Pattanaik & Montgomery, 2010). $\Delta rcaF$ and $\Delta rcaC$ mutants also showed lower growth during increasing periods of time under iron-limited conditions, which was more highly impacted under RL than GL, similar to WT (Fig. 1e, f and Fig. 1g, h, respectively). Significant differences in the growth of WT, $\Delta rcaF$ and $\Delta rcaC$ strains were observed by 6 days of exposure to iron limitation irrespective of light condition. However, even after 15 days, the $\Delta rcaE$ mutant showed only a slight decrease in growth in iron-limited medium, i.e. a 0.15-fold decrease in GL or 0.17-fold decrease in RL (Fig. 1c, d), compared with other strains (WT, 0.4-fold decrease for GL and 0.7-fold decrease for RL; $\Delta rcaF$, 0.5-fold decrease for GL and 0.65-fold decrease for RL; and $\Delta rcaC$, 0.42-fold decrease for GL and 0.6-fold decrease for RL).

The intracellular iron contents of cells grown in iron-replete or iron-limited conditions were measured to determine whether intracellular iron levels were correlated with the observed differences in growth. All of the strains exhibited lower intracellular levels of iron during growth under iron-limited conditions than in iron-replete medium (Table 1). We determined that GL-grown WT cells accumulated more iron than WT cells grown under RL (Table 1). This observation may be associated with the ability of GL-grown WT cells to show partial resistance to iron limitation relative to RL-grown WT cells. Notably, the $\Delta rcaE$ mutant accumulated lower levels of iron than WT under both (Table 1), although the cells showed essentially no growth impairments in iron-limited medium under either GL or RL (Fig. 1c, d). The $\Delta rcaF$ and $\Delta rcaC$ strains exhibited iron levels that were generally lower than WT and the $\Delta rcaE$ mutant in iron-replete medium under GL (Table 1), although the growth of the $\Delta rcaF$ and $\Delta rcaC$ strains was nearly identical to WT (Fig. 1), indicating that the differences in growth cannot be explained by the differences in intracellular iron content alone.

F. diplosiphon cells grown in iron-limited conditions exhibit light-dependent differences in the regulation of photosynthetic pigment accumulation

chl*a* and PBPs, including allophycocyanin (AP), phycocyanin (PC) and phycoerythrin (PE), were extracted from

F. diplosiphon strains grown in iron-limited or iron-replete medium for 15 days under GL and RL. chl*a* levels were significantly reduced ($P<0.0001$) in all the strains grown in iron-limited medium compared with iron-replete medium, independent of light condition (Table 2). Under iron-replete conditions, none of the strains showed any statistical difference in the amount of chl*a* under GL versus RL (Table 2), as previously observed for WT *F. diplosiphon* cells (Singh & Montgomery, 2011). Notably, in iron-limited conditions chl*a* content was significantly reduced in both GL- and RL-grown cells in all the strains, though the reduction for the $\Delta rcaE$ mutant in iron-limited medium under GL was less than that observed for all other strains and light conditions (Table 2).

AP accumulation was reduced significantly by iron-limited growth in WT, but only under RL (Table 2). By comparison, AP accumulation was decreased significantly in both $\Delta rcaF$ and $\Delta rcaC$ mutants under both RL and GL in response to iron limitation (Table 2). Notably, no significant change in AP levels was observed for the *rcaE* mutant in iron-limited conditions under either GL or RL (Table 2).

PC accumulation in cells grown in iron-limited medium varied in each strain in comparison to iron-replete medium. Under RL, WT, $\Delta rcaE$, $\Delta rcaF$ and $\Delta rcaC$ strains all exhibited significantly decreased PC accumulation under iron-limited conditions compared to cultures grown in iron-replete medium (Table 2). However, the fold reduction observed for the $\Delta rcaE$ under RL and iron limitation was much less than that observed for WT (Table 2). Under GL, iron limitation had a significant impact on PC accumulation only in the $\Delta rcaF$ mutant, (Table 2). In general, the $\Delta rcaE$ mutant accumulated higher AP and PC than other strains, independent of the presence or absence of iron in the medium (Table 2). The higher accumulation of PC in this mutant in iron-replete medium had been previously reported (Singh & Montgomery, 2011).

PE accumulation was higher in $\Delta rcaF$ and $\Delta rcaC$ mutants as compared to WT and the $\Delta rcaE$ mutant under both light conditions in iron-replete medium (Table 2). A significant decrease in PE accumulation was observed with iron-limited growth under either GL or RL in WT and the $\Delta rcaF$ and $\Delta rcaC$ mutants (Table 2). PE accumulation showed a significant decrease in the $\Delta rcaE$ mutant grown in iron-limited medium under GL, but not under RL (Table 2).

F. diplosiphon cells exhibit light-regulated accumulation of ROS under iron limitation

Levels of ROS are increased in cyanobacteria during photosynthesis and respiration when light absorption exceeds the photosynthetic capacity of the cell, and numerous stress factors have the potential to increase the production of ROS in photosynthetic cells (for review see Latifi *et al.*, 2009). *F. diplosiphon* WT, $\Delta rcaF$ and $\Delta rcaC$ strains produced higher amounts of ROS under
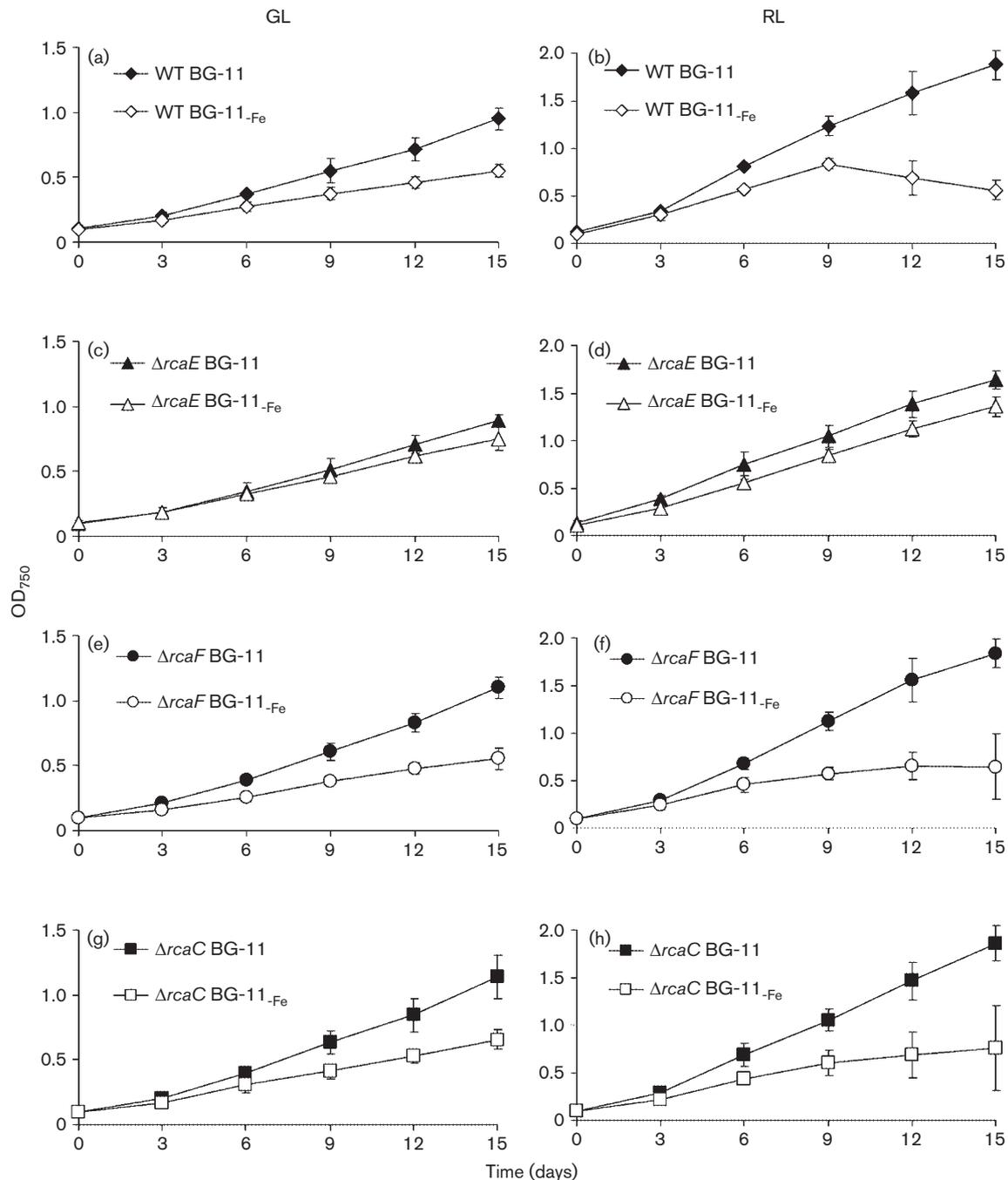
Fig. 1. Growth analyses of *F. diplosiphon* strains grown in iron-replete (BG-11) and iron-limited (BG-11$_{-Fe}$) culture medium under GL or RL conditions. (a, b) SF33 WT pigmentation strain; (c, d) ΔrcaE mutant; (e, f) ΔrcaF mutant; (g, h) ΔrcaC mutant. Growth of cultures was measured as OD$_{750}$ at 3-day intervals. Each point represents the mean (±SD) for at least three independent biological replicates.

iron-limited conditions compared with iron-replete conditions (Fig. 2a). Higher ROS generation also was detected in these three strains under RL compared with GL (Fig. 2a). In response to iron limitation, WT cells generally produced a higher amount of ROS (15-fold increase under GL, 83-fold increase under RL) than did ΔrcaF (15-fold increase under GL, 39-fold increase under RL) and ΔrcaC mutants (12-fold increase under GL, 20-fold increase under RL) (Fig. 2a). Markedly, no increase in ROS levels was observed for the ΔrcaE strain in response to iron limitation (Fig. 2a).

Table 1. Iron-content analysis in *F. diplosiphon* SF33 WT pigmentation and *rca* mutant strains grown in iron-replete (BG-11) or iron-limited (BG-11$_{-Fe}$) culture medium under GL or RL conditions

Iron content was measured by ICP-OES in two replicate samples. Numbers are means ($\pm$SE). DW, dry weight.

Strain	Medium	Iron content [μg Fe (mg DW) $^{-1}$]	
		GL	RL
WT	+Fe	2.2 ($\pm$0.9)	1.0 ($\pm$0.5)
	−Fe	0.65 ($\pm$0.1)	0.3 ($\pm$0.05)
Δ*rcaE*	+Fe	1.8 ($\pm$0.2)	1.0 ($\pm$0.02)
	−Fe	0.5 ($\pm$0.1)	0.6 ($\pm$0.1)
Δ*rcaF*	+Fe	1.0 ($\pm$0.1)	1.2 ($\pm$0.04)
	−Fe	0.6 ($\pm$0.1)	0.35 ($\pm$0.05)
Δ*rcaC*	+Fe	1.2 ($\pm$0.1)	1.0 ($\pm$0.01)
	−Fe	0.7 ($\pm$0.2)	0.4 ($\pm$0.05)

Transcriptomic responses to iron limitation indicate RcaE- and light-regulated cellular responses

To gain insights into the mechanistic bases of the greater resistance to iron limitation in WT cells under GL and Δ*rcaE* mutant cells in regard to growth and the generation of ROS independent of external light conditions, we conducted transcriptomic analyses to assess differences in gene expression, particularly for genes encoding proteins known to impact cellular responses to iron limitation and oxidative stress. Expression of two genes homologous to a recognized iron-permease-encoding gene, *FTR1*, was upregulated, as expected, in cells grown in iron-limited medium under both GL and RL (Table 3). We also identified a number of genes related to cellular responses to ROS that were differentially expressed in RL versus GL and/or in WT versus the Δ*rcaE* mutant (Table 3). We identified two annotated Mn/Fe SOD-encoding genes, one of which was downregulated in iron-limited media (i.e. Ava_0963 homologue), and both of which accumulated to higher levels in the Δ*rcaE* mutant, which is largely resistant to iron limitation (Table 3). A catalase homologue, which may require iron as a cofactor, was downregulated in iron-limited medium; yet accumulated to higher levels in the Δ*rcaE* mutant, which shows resistance to iron limitation (Table 3). We also identified a possible ROS-mitigating peroxidase, which was significantly upregulated in WT cells, that exhibited higher ROS levels (Fig. 2a). This peroxidase was induced to lower levels in the non-ROS-accumulating Δ*rcaE* mutant (Table 3).

Ferritin-like proteins have roles in iron storage (Keren *et al.*, 2004), as well as organismal responses to oxidative stress in cyanobacteria (Ekman *et al.*, 2014). We thus assessed the impact of iron limitation on a number of ferritins that we annotated in the RNa-Seq data. We identified six annotated ferritin or ferritin-like proteins, five of which were downregulated in response to iron limitation and which accumulated to higher levels in the Δ*rcaE* mutant (Table 3). A TonB protein, which we previously showed impacts cellular morphology, but had little impact on cell growth rates in response to iron limitation based on analyses of a Δ*tonB* mutant (Pattanaik & Montgomery, 2010), accumulated to higher levels in iron-limited conditions (Table 3).

Table 2. Photosynthetic pigment levels in *F. diplosiphon* SF33 WT pigmentation and *rca* mutant strains grown in iron-replete (BG-11) or iron-limited (BG-11$_{-Fe}$) culture medium under GL or RL conditions

Values in parentheses indicate SD from at least three independent biological replicates.

Strain	Medium	Light	chl*a* (μg ml^{-1})†	AP (μg ml^{-1})†	PC (μg ml^{-1})†	PE (μg ml^{-1})†
WT	+Fe	RL	0.35 (0.04)	1.09 (0.54)	2.35 (1.0)	0.34 (0.2)
		GL	0.30 (0.1)	0.62 (0.17)	0.53 (0.08)	2.95 (0.38)
	−Fe	RL	0.1 (0.015)***	0.38 (0.15)**	1.06 (0.09)**	0.15 (0.09)*
		GL	0.12 (0.1)***	0.47 (0.24)	0.48 (0.10)	2.33 (0.28)**
Δ*rcaE*	+Fe	RL	0.4 (0.1)	1.65 (0.43)	2.19 (0.29)	2.69 (0.63)
		GL	0.4 (0.1)	2.18 (0.43)	2.95 (0.40)	3.02 (0.36)
	−Fe	RL	0.17 (0.04)***	1.33 (0.31)	1.88 (0.25)*	2.34 (0.40)
		GL	0.3 (0.01)***	2.06 (0.27)	2.74 (0.29)	2.43 (0.19)***
Δ*rcaF*	+Fe	RL	0.36 (0.05)	1.13 (0.31)	0.94 (0.17)	4.19 (0.59)
		GL	0.35 (0.01)	1.38 (0.38)	0.97 (0.08)	4.91 (0.35)
	−Fe	RL	0.14 (0.02)***	0.36 (0.13)***	0.49 (0.16)***	1.57 (0.74)***
		GL	0.16 (0.01)***	0.90 (0.21)**	0.72 (0.05)***	3.14 (0.50)***
Δ*rcaC*	+Fe	RL	0.32 (0.03)	0.93 (0.28)	0.72 (0.18)	3.53 (0.51)
		GL	0.32 (0.1)	1.14 (0.32)	0.81 (0.22)	4.55 (0.85)
	−Fe	RL	0.11 (0.02)***	0.45 (0.13)***	0.52 (0.11)*	1.79 (0.50)***
		GL	0.16 (0.01)***	0.82 (0.33)*	0.67 (0.08)	2.95 (0.17)***

†*P* value determined using unpaired two-tailed Student's *t*-test: *$P<0.05$; **$P<0.005$; ***$P<0.0005$.
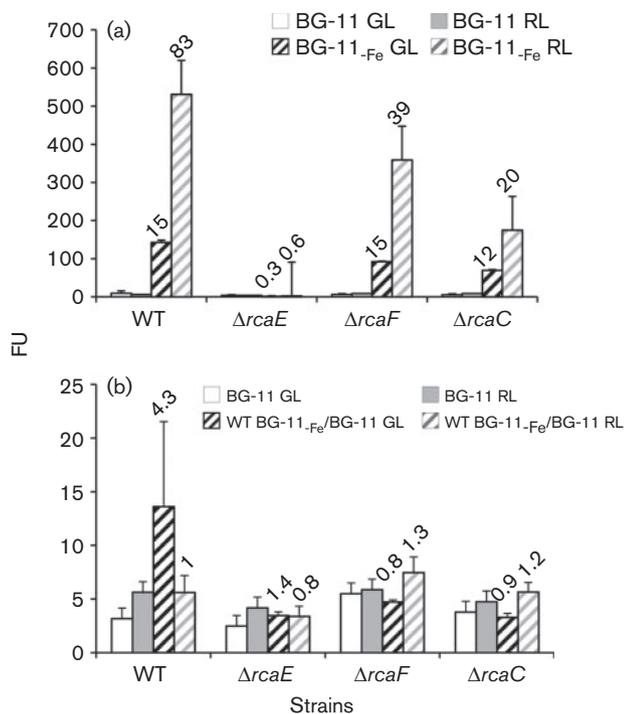
Fig. 2. ROS accumulation analysis of *F. diplosiphon* SF33 WT pigmentation strain, and Δ*rcaE* mutant, Δ*rcaF* mutant and Δ*rcaC* mutant strains grown in iron-replete (BG-11), iron-limited (BG-11$_{-Fe}$) or iron-limited cultures transferred to iron-replete (BG-11$_{-Fe}$/BG-11) culture medium under GL or RL conditions. Each bar represents the mean (±SE) for at least four independent biological replicates. The numbers above the bars indicate fold increase of ROS measured in fluorescence units (FU) in cells grown in iron-limited conditions relative to the same strain grown in iron-replete or iron-recovery conditions. (a) iron-replete versus iron-limited conditions. (b) iron-replete versus iron-recovered conditions.

Enzymic responses to mitigate iron limitation-associated oxidative stress

To assess further the mechanism by which WT cells resist iron limitation under GL and Δ*rcaE* cells show limited responses to iron limitation independent of light conditions, we assessed the accumulation and activity of SOD enzymes in these cells. We tested accumulation of FeSOD for WT and Δ*rcaE* strains grown in iron-replete or iron-limited medium under both GL and RL growth conditions. Using native PAGE to assay for SOD enzyme activity, we determined that FeSOD activity and protein content were higher under replete conditions compared with iron-limited conditions in WT cells under both light conditions and in Δ*rcaE* cells in RL (Fig. 3). Δ*rcaE* cells showed similar levels of FeSOD under iron-limited and replete conditions in GL (Fig. 3). To determine the type of SOD enzyme accumulating in *F. diplosiphon*, we treated protein extracts with a Cu/ZnSOD enzyme inhibitor, i.e. KCN, or a FeSOD inhibitor, i.e. H$_2$O$_2$. Treatment with the FeSOD inhibitor resulted in a lack of detection of SOD activity in WT and Δ*rcaE* samples (data not shown), confirming the presence of a FeSOD enzyme in *F. diplosiphon* samples under specific light and growth media conditions. However, treatment with the Cu/ZnSOD inhibitor had no impact on the detection of SOD activity in either WT or Δ*rcaE* samples (data not shown). Furthermore, immunoblot analyses with anti-MnSOD or anti-Cu/ZnSOD antibodies did not result in the detection of a band in *F. diplosiphon* samples (data not shown).

F. diplosiphon cells grown in iron-limited conditions exhibit morphological differences

The cellular morphology of WT *F. diplosiphon* is known to be affected by iron limitation during the process of CCA (Pattanaik & Montgomery, 2010). We previously reported that WT cells are larger and exhibit vacuolation under iron-limited conditions irrespective of external light conditions (Pattanaik & Montgomery, 2010). To determine whether any of the *rca* mutants exhibit specific morphological changes under iron-limited conditions compared with iron-replete conditions, we conducted CLSM analyses of cells grown in both light conditions in iron-replete or iron-limited medium. Similar to prior responses noted for WT (compare Fig. 4a, b with Fig. 4c, d; Pattanaik & Montgomery, 2010), we observed iron-limitation-induced vacuolation in both Δ*rcaF* and Δ*rcaC* mutants in both GL and RL (compare Fig. 4i, j with Fig. 4k, l and Fig. 4m, n with Fig. 4o, p, respectively). Notably, a Δ*rcaE* mutant showed virtually no morphological changes in response to iron-limited conditions, particularly under GL conditions, though limited vacuolation was detected in Δ*rcaE* cells subjected to iron limitation under RL (compare Fig. 4e, f with Fig. 4 g, h).

Response of *F. diplosiphon* cells after iron recovery

We adapted cultures grown in iron-limited conditions to iron-replete medium for 15 days to determine whether the effects observed under iron-limited growth were reversible or whether permanent changes were associated with iron limitation. WT cells showed full iron recovery under GL and RL conditions based on growth analyses (Fig. 5a, b). The Δ*rcaE* mutant showed similar growth under iron-recovery conditions under GL and RL as observed for the strain under iron limitation (Fig. 5c, d). Both Δ*rcaF* and Δ*rcaC* mutants showed iron recovery under both GL and RL, though the recovery was slightly more complete under RL in both strains (Fig. 5e, f, g, h).

WT and all three mutants showed similar chl*a* accumulation in response to iron limitation relative to iron recovery (Table 4). The amount of each PBP was also measured after iron recovery in all strains. All strains largely recovered PBP levels that were similar to iron-replete cultures (Table 4). However, WT did not fully recover PC or PE levels by 15 days under GL, or AP, PC or PE levels by 15 days under RL (Table 4), whereas the Δ*rcaF* mutant did not fully recover AP, PC or PE levels by 15 days under GL or RL
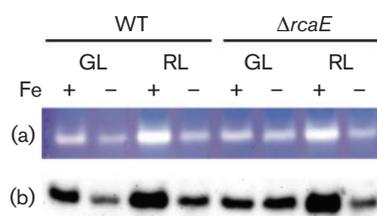
Table 3. RNA sequencing data from *F. diplosiphon* SF33 WT pigmentation and *rcaE* mutant strains grown in iron-replete (BG-11) or iron-limited (BG-11$_{-Fe}$) culture medium under GL or RL conditions

Read	Annotation	*Ava* homologue*	Sample	No. of reads				Fold change†		*P* value‡	
				WT		Δ*rcaE*		WT	Δ*rcaE*	WT	Δ*rcaE*
				GL	RL	GL	RL				
4983	*FTR1*	Ava_1763	+Fe	333	303	329	719	0.9	2.2	0.81	8×10^{-6}
			−Fe	1155	855.5	523	1101	0.7	2.1	0.26	0.04
6424	*FTR1*	Ava_1763	+Fe	11	20	17	18	1.9	1.1	0.04	0.77
			−Fe	153	210	201	168	1.4	0.8	0.27	0.42
5210	Mn/Fe SOD	Ava_1445	+Fe	498	369	736	500	0.7	0.7	0.28	0.08
			−Fe	539	461	850	538	0.85	0.6	0.53	0.85
6664	Mn/Fe SOD	Ava_0963	+Fe	2258	1873	2033	3886	0.8	1.9	0.52	0.0006
			−Fe	635	697	1377	1895	1.1	1.4	0.77	0.42
4666	Mn catalase	Ava_3821	+Fe	241	511	401	946	2.1	2.4	0.03	3×10^{-6}
			−Fe	108	203	158	321	1.9	2.0	0.03	0.15
6522	Peroxidase	Ava_4196	+Fe	12	24	19	11	2.0	0.6	0.03	0.20
			−Fe	247	226	143	178	0.9	1.2	0.95	0.56
3271	Ferritin/Dps	Ava_2868	+Fe	377	501	593	1009	1.3	1.7	0.32	0.002
			−Fe	261	423	471	557	1.6	1.8	0.08	0.96
4510	Ferritin/Dps	Ava_0759	+Fe	80	86	142	222	1.1	1.6	0.97	0.02
			−Fe	33	44	69	60	1.3	0.9	0.49	0.65
4983	Ferritin/Dps	Ava_1762	+Fe	1226	3291	1095	2585	2.7	2.3	0.01	1×10^{-5}
			−Fe	2423	2566	2075	2412	1.1	1.2	0.84	0.80
1685	Ferritin/Dps	Ava_1894	+Fe	2061	2999	2598	4987	1.5	1.9	0.29	0.0005
			−Fe	1716	2175	1987	3615	1.3	1.8	0.42	0.21
6350	Ferritin-like/ Dps	Ava_4423	+Fe	1067	1404	1758	4987	1.3	2.3	0.66	4×10^{-5}
			−Fe	550	506	1234	1174	0.9	0.95	0.71	0.65
4667	Ferritin-like/ Mn catalase	Ava_3821	+Fe	241	511	410	916	2.1	2.2	0.03	1×10^{-5}
			−Fe	107	203	160	318	1.9	2.0	0.03	0.17
408	TonB	Ava_2295	+Fe	74	131	131	93	1.8	0.68	0.01	0.15
			−Fe	1197	1336	957	669	1.1	0.70	0.71	0.20

*ORFs were compared against *A. variabilis* (*Ava*) ATCC 29413 annotated proteins using BLASTX with a cut-off *e*-value of 0.0001 to determine the *Ava* homologue.

†Fold change: differential expression analysis between two light treatments was carried out for each strain.

‡*P* value: the significance value was calculated for RL versus GL counts for each strain.

Fig. 3. Assay of FeSOD activity and protein accumulation of SF33 WT pigmentation strain and Δ*rcaE* mutant. (a) Native PAGE assay of protein extracts for FeSOD activity. Protein extracts of *F. diplosiphon* SF33 WT pigmentation strain or Δ*rcaE* mutant strain grown in iron-replete (+Fe) or iron-limited (−Fe) culture media under GL or RL conditions. Regions with SOD activity are indicated by white bands on a darker blue background. (b) Immunoblot analysis for detection of FeSOD protein accumulation.

(Table 4), though levels were significantly greater during iron recovery than in iron-limited conditions in all cases. The Δ*rcaC* mutant failed to recover fully AP levels under RL, yet recovered higher levels of PC under GL and RL, and higher PE and AP under GL (Table 4). Levels of pigments in the Δ*rcaE* mutant were higher or not statistically different during recovery growth compared with iron-limited growth, with the exception of PE under RL, which was significantly less in recovery growth than in replete conditions (Table 4).

All strains produced less ROS after iron recovery than under iron-limited conditions (Fig. 2b). However, under GL, iron-recovered WT cells still produced a 4.3-fold higher amount of ROS than the iron-replete WT cells (Fig. 3b). This observation indicates that these cells were largely, but not fully, recovered from iron stress, in general agreement with the response observed for pigment levels in this strain (Table 4). Morphologically, all of the strains, with the exception of
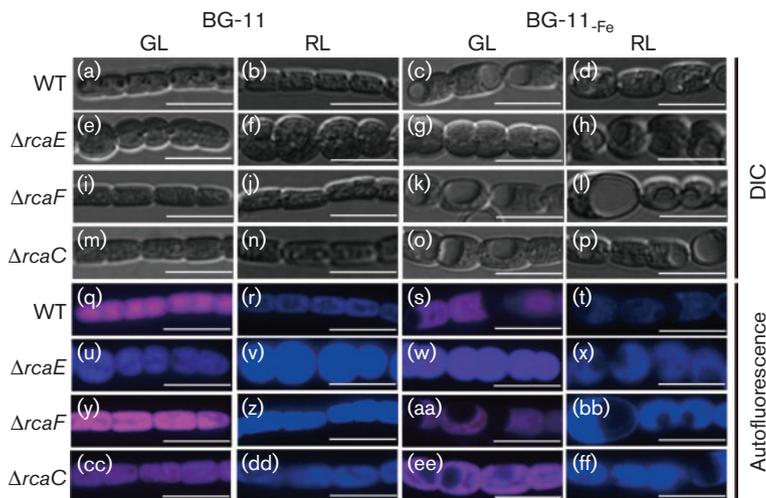
Fig. 4. CLSM analyses of cellular morphology of *F. diplosiphon* strains grown in iron-replete (BG-11) and iron-limited (BG-11$_{-Fe}$) culture medium under GL or RL conditions. Representative optical slices from a Z-series of DIC images (a–p) and maximum-intensity projection of PBP autofluorescence images (q–ff) of SF33 WT pigmentation strain (a–d and q–t), and Δ*rcaE* mutant (e–h and u–x), Δ*rcaF* mutant (i–l and y–bb) and Δ*rcaC* mutant (m–p and cc–ff) strains. All images were acquired with a ×40 oil objective with ×2 zoom. Bars, 10 μm.

the Δ*rcaF* mutant grown under RL, lacked vacuolation after recovery in iron-replete medium for 15 days, indicating a largely reversible effect of iron limitation on the cells (Fig. 6).

DISCUSSION

Iron limitation has a negative impact on photosynthesis, but also on other iron-dependent processes at the physiological and cellular levels. In this study, we report the impact of iron limitation on WT and mutant strains of *F. diplosiphon* during the process of CCA. The well-characterized process of CCA is known to be controlled by a complex, photoreceptor-based phosphorelay regulatory system (Gutu & Kehoe, 2012; Kehoe & Gutu, 2006). RcaE is the photoreceptor, responsive to RL and GL, and immediately after RcaE, a small response regulator RcaF acts in the signalling cascade, and RcaC is a DNA-binding response regulator that functions in the pathway after RcaF (Gutu & Kehoe, 2012).

We observed light- and genotype-specific responses to iron limitation in *F. diplosiphon*. Decreased growth and lower levels of all PBPs were observed in the iron-limited *F. diplosiphon* WT pigmentation strain under RL, whereas a lesser impact on growth and a reduction in chl*a* and PE levels were observed in WT cells grown in iron-limited conditions under GL (Fig. 1, Table 2). Notably, two strains of *Prochlorococcus*, which grow in distinct depths, and thus light environments, exhibit distinct iron requirements (Thompson *et al.*, 2011). *Prochlorococcus* ecotype MED4 grows at the surface, which is enriched for RL wavelengths, and requires higher iron concentrations to support growth than ecotype MIT9313, which grows in deep parts of the ocean where overall light levels are low and red wavelengths are depleted (Thompson *et al.*, 2011). In WT-pigmented *F. diplosiphon* under RL conditions, chl*a*, AP and PC are capable of absorbing RL for photosynthesis. Under conditions in which PBP levels are reduced, chl*a* alone can continue to absorb light for photosynthesis (Lemasson *et al.*, 1973). However, chl*a* does not directly absorb GL. Thus,

iron-limited, RL-grown cells can greatly reduce PBP levels and chlorophyll synthesis to compensate for reduced iron availability, resulting in lower overall photosynthetic pigment levels, yet cells can presumably survive by using a pool of photosynthetic pigments to absorb sufficient light for photosynthesis. However, as PE is the primary light-absorbing photosynthetic protein under GL (Campbell, 1996), a fully intact PBS and moderately high levels of PE must be maintained to support photosynthesis under GL. A significant reduction in PE levels under iron limitation together with no significant difference in the levels of PC or AP (Table 2) does, however, suggest that shorter rods are present. This reduction in rod length in iron-limited medium may allow cells to spare iron to some degree while still maintaining PE-rich rods in functional PBSs for supporting photosynthesis and growth in GL. We believe that the minor impact of iron limitation on photosynthetic pigments that we observed under GL for WT cells reflects this biological necessity, and suggests a GL-dependent mechanism for resisting severe depletion of photosynthetic pigments in response to iron limitation in *F. diplosiphon*.

During iron limitation, one of the first responses of cyanobacteria is to degrade the PBSs leading to chlorosis, as discussed before, and as a protective mechanism many of these organisms synthesize proteins that function around PSI and PSII to reduce electron flow, which leads to reduced ROS formation (Boekema *et al.*, 2001; Ferreira & Straus, 1994; Lax *et al.*, 2007). However, when iron limitation in cyanobacterial cells becomes severe, excess light energy cannot be utilized by the modified or degraded PBSs, and leads to the formation of ROS and resultant oxidative stress (Latifi *et al.*, 2009; Michel & Pistorius, 2004). Iron-limitation and oxidative stress responses in cyanobacteria are therefore closely linked (Latifi *et al.*, 2009). An additional contributor to increased ROS levels under iron limitation may be the reduced accumulation and/or activity of iron-dependent ROS scavengers or detoxifying enzymes (Michel & Pistorius, 2004). In our study, higher ROS production was detected in cells grown under iron-limited conditions and was higher
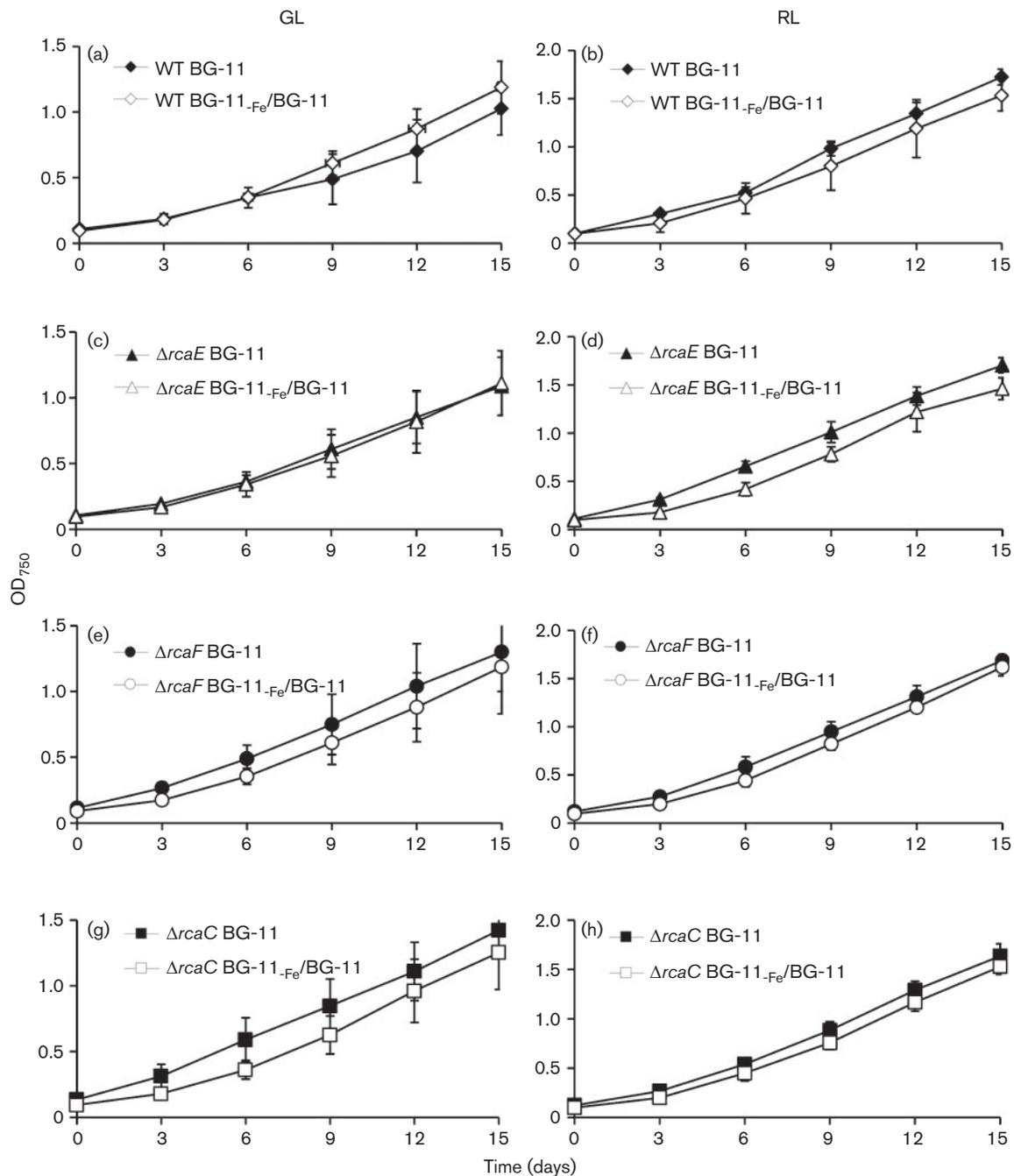
Fig. 5. Iron-recovery growth analyses of *F. diplosiphon* strains grown in iron-replete (BG-11) and iron-limited cultures transferred to iron-replete (BG-11$_{-Fe}$/BG-11) culture medium under GL or RL conditions. (a, b) SF33 WT pigmentation strain; (c, d) Δ*rcaE* mutant; (e, f) Δ*rcaF* mutant; and (g, h) Δ*rcaC* mutant. Growth of cultures was measured as OD$_{750}$ at 3-day intervals. Each point represents the mean (±SD) for at least three independent biological replicates.

still under RL than GL. (Fig. 2). The conditions under which *F. diplosiphon* accumulates higher ROS levels, i.e. RL and iron limitation, correspond to those under which the cells show a more severely reduced growth response to iron limitation (Fig. 1) and a reduced accumulation of FeSOD (Fig. 3). Thus, the higher accumulation of ROS under RL and

iron limitation may reflect the greater impact of iron limitation on ROS-detoxifying enzymes that require iron cofactors under this condition (Michel & Pistorius, 2004).

An increase in transcript levels in response to iron limitation was reported in different organisms and was

Table 4. Iron-recovery photosynthetic pigment levels in *F. diplosiphon* SF33 WT pigmentation and *rca* mutant strains grown in iron-replete (BG-11) or iron-limited cultures transferred to iron-replete (BG-11$_{-Fe}$/BG-11) culture medium under GL or RL conditions

Values in parentheses indicate SD from at least three independent biological replicates.

Strain	Medium	Light	chl*a* (µg ml^{-1})†	AP (µg ml^{-1})†	PC (µg ml^{-1})†	PE (µg ml^{-1})†
WT	+Fe	RL	0.39 (0.06)	1.41 (0.01)	2.69 (0.04)	0.38 (0.01)
		GL	0.33 (0.11)	0.81 (0.08)	0.74 (0.04)	3.61 (0.08)
	−Fe/+Fe	RL	0.37 (0.05)	1.07 (0.14)***	2.14 (0.16)***	0.30 (0.03)***
		GL	0.35 (0.02)	0.75 (0.07)	0.62 (0.03)***	3.03 (0.01)***
Δ*rcaE*	+Fe	RL	0.45 (0.06)	1.80 (0.05)	2.28 (0.11)	3.07 (0.11)
		GL	0.40 (0.04)	1.99 (0.11)	3.03 (0.08)	2.71 (0.09)
	−Fe/+Fe	RL	0.50 (0.055)	1.81 (0.06)	2.31 (0.07)	2.96 (0.095)*
		GL	0.42 (0.02)	2.26 (0.07)***	3.26 (0.04)***	2.98 (0.04)***
Δ*rcaF*	+Fe	RL	0.38 (0.04)	1.35 (0.04)	1.07 (0.02)	4.77 (0.09)
		GL	0.36 (0.04)	1.64 (0.14)	1.20 (0.02)	5.56 (0.06)
	−Fe/+Fe	RL	0.42 (0.04)	1.20 (0.03)**	0.95 (0.02)***	4.45 (0.03)***
		GL	0.32 (0.08)	1.41 (0.08)***	1.07 (0.04)***	4.83 (0.05)***
Δ*rcaC*	+Fe	RL	0.36 (0.065)	1.04 (0.06)	0.77 (0.06)	3.79 (0.12)
		GL	0.35 (0.04)	1.23 (0.11)	0.92 (0.03)	4.54 (0.14)
	−Fe/+Fe	RL	0.39 (0.04)	0.97 (0.05)*	0.81 (0.02)*	3.82 (0.05)
		GL	0.34 (0.04)	1.38 (0.12)*	1.09 (0.07)***	4.98 (0.15)***

†*P* value determined using unpaired two-tailed Student's *t*-test: **P*<0.05; ***P*<0.005; ****P*<0.0005.

mostly associated with oxidative stress (Latifi *et al.*, 2009). The results we obtained from transcriptomics and SOD protein analysis provide strong evidence that *F. diplosiphon* cells exhibit light-dependent differences for actively adapting to limitation in external iron availability. The severe reduction in FeSOD activity under iron limitation in WT cells under RL correlates with the lower growth of these cells. The reduction in fold change of FeSOD activity under iron limitation in WT cells under GL, and more notably in Δ*rcaE* cells under both light conditions (Fig. 3), provides strong evidence that these cells are not experiencing the same level of internal iron deficiency as WT under RL and iron-limited growth conditions. These observations indicate that WT cells growing under GL and iron limitation have mechanisms for avoiding iron deficiency, and that RcaE is a central player in the response of cells to iron limitation, as in its absence cells show very limited growth responses to iron limitation. Notably, transcripts of ferritin-like genes in *F.*

diplosiphon, although reduced in iron-limited growth conditions for five of six such genes, accumulated to higher levels in a Δ*rcaE* mutant (Table 3). This suggests that Δ*rcaE* cells have a higher capacity for storing iron, which may be associated with the iron-limitation resistant phenotype observed for these cells. Furthermore, as soluble FeSOD is involved in protection against oxidative stress in closely related cyanobacteria, including *Nostoc* sp. PCC 7120 (Regelsberger *et al.*, 2004), and its light-dependent accumulation is different in RcaE-deficient cells than WT (Fig. 4), RcaE appears central to regulation of light- and nutrient-deficient oxidative stress responses in *F. diplosiphon*. We have observed a prior association of RcaE accumulation in cells with the photoregulation of ROS levels (Singh & Montgomery, 2012).

A Δ*rcaE* mutant exhibited very specific light and nutrient effects on growth and regulation of PC and PE levels
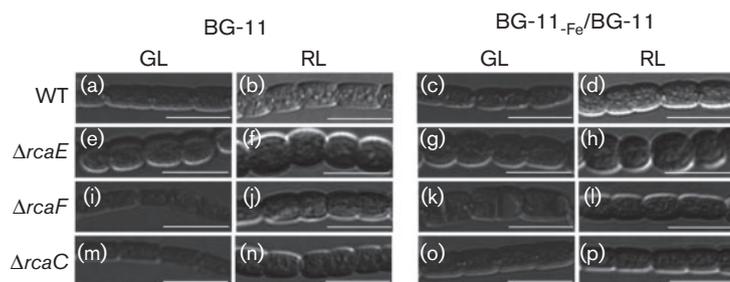
Fig. 6. CLSM analyses of cellular morphology of *F. diplosiphon* strains grown in iron-replete (BG-11) and iron-limited cultures transferred to iron-replete (BG-11$_{-Fe}$/BG-11) culture medium under GL or RL conditions. Representative optical slices from a Z-series of DIC images of SF33 WT pigmentation strain (a–d), and Δ*rcaE* mutant (e–h), Δ*rcaF* mutant (i–l) and Δ*rcaC* mutant (m–p) strains. All images were acquired with a ×40 oil objective with ×2 zoom. Bars, 10 µm.

compared with WT, Δ*rcaF* and Δ*rcaC* mutant strains (Fig. 1, Table 2). Minor differences in the growth of the Δ*rcaE* mutant cells under either GL or RL were detected under iron limitation (Fig. 1), indicating a high survival response under iron-limited conditions for this strain. The only major reductions in pigment levels observed for the Δ*rcaE* mutant in response to iron limitation were for chl*a* levels under RL and GL, PE under GL and PC under RL (Table 2). However, the reductions were much less in each of these cases than those observed for other strains (Table 2). These results provide strong evidence that the Δ*rcaE* mutant is largely resistant to iron limitation. These differences are not due to Δ*rcaE* mutant cells accumulating more iron than WT (Table 1), and thus strongly support a central regulatory role for RcaE in the organismal response to iron limitation.

Iron limitation impacts morphology in several organisms, including cyanobacteria. In our study, we observed vacuoloation in WT, Δ*rcaF* and Δ*rcaC* cells in response to iron stress under both GL and RL (Fig. 4). However, the Δ*rcaE* strain did not show any specific morphological change in response to iron limitation, or induction of vacuolation, particularly under GL (Fig. 4). The induction of vacuolation in *F. diplosiphon* thus appears to be associated with increased levels of oxidative stress, providing additional evidence of a resistance of the Δ*rcaE* strain to iron limitation-induced stress.

Once iron-limited cells were subjected to iron recovery in iron-replete medium, the cells returned to a phenotype that largely reflects WT pigmentation and morphology. This observation suggests that *F. diplosiphon* cells have an ability to regain their photosynthetic pigments and growth rates in response to iron recovery (Fig. 5, Table 4). Iron-recovered cells also largely lacked stress-related vacuolation (Fig. 6). Our observations are supported by previous reports confirming morphological rearrangements and re-establishment of photosynthetic pigment levels in other cyanobacteria after iron recovery (Hardie *et al.*, 1983a, b; Sherman & Sherman, 1983).

RcaE and its cognate response regulators RcaF and RcaC have central roles in the photoregulation of pigmentation and cellular morphology under GL and RL in *F. diplosiphon*, and RcaE impacts the photoregulation of ROS levels (Fig. 2; Singh & Montgomery, 2012). Here, we report a regulatory role for RcaE in the light-dependent, iron-limited generation of ROS. Furthermore, the results described here support the conclusion that RcaE is critical for photoregulation of iron-acclimation responses, as a Δ*rcaE* mutant shows little to no response to iron limitation independent of the external light conditions. This involvement of RcaE appears to occur independently of RcaF and RcaC effector functions, as mutants harbouring insertional mutations in either *rcaF* or *rcaC* still exhibit light-dependent iron limitation responses. RcaE has been shown to function independently of RcaF and RcaC in other responses, most recently in the regulation of cellular morphology under GL (Bordowitz *et al.*, 2010).

We propose that RcaE regulates photoadaptation to iron limitation under both GL and RL in *F. diplosiphon*. However, the exact mechanisms by which RcaE mediates these processes will require additional inquiry. Elucidation of the regulatory mechanisms employed by photosynthetic organisms for balancing the energy demands of photosynthesis with the energy costs of responding to environmental variations in light and nutrient availability requires further investigation as few environmental sensors, such as RcaE, have been linked to iron homeostasis regulation. Additional analyses of the effects of iron limitation will provide insight into how light and nutrient availability interact to fine-tune resource allocation in organisms, an area that is currently underinvestigated.

ACKNOWLEDGEMENTS

REFERENCES

Anders, S. & Huber, W. (2010). Differential expression analysis for sequence count data. *Genome Biol* **11**, R106.

Beauchamp, C. & Fridovich, I. (1971). Superoxide dismutase: improved assays and an assay applicable to acrylamide gels. *Anal Biochem* **44**, 276–287.

Behrenfeld, M. J., Bale, A. J., Kolber, Z. S., Aiken, J. & Falkowski, P. G. (1996). Confirmation of iron limitation of phytoplankton photosynthesis in the equatorial Pacific Ocean. *Nature* **383**, 508–511.

Benešová, J., Ničková, K., Ferimazova, N. & Štys, D. (2000). Morphological and physiological differences in *Synechococcus elongatus* during continuous cultivation at high iron, low iron, and iron deficient medium. *Photosynthetica* **38**, 233–241.

Bhaya, D., Schwarz, R. & Grossman, A. R. (2000). Molecular responses to environmental stresses. In *Ecology of Cyanobacteria: Their Diversity in Time and Space*, pp. 397–442. Edited by B. A. Whitton & M. Potts. Dordrecht: Kluwer.

Boekema, E. J., Hifney, A., Yakushevska, A. E., Piotrowski, M., Keegstra, W., Berry, S., Michel, K. P., Pistorius, E. K. & Kruip, J. (2001). A giant chlorophyll-protein complex induced by iron deficiency in cyanobacteria. *Nature* **412**, 745–748.

Bordowitz, J. R. & Montgomery, B. L. (2008). Photoregulation of cellular morphology during complementary chromatic adaptation

requires sensor-kinase-class protein RcaE in *Fremyella diplosiphon*. *J Bacteriol* **190**, 4069–4074.

Bordowitz, J. R. & Montgomery, B. L. (2010). Exploiting the autofluorescent properties of photosynthetic pigments for analysis of pigmentation and morphology in live *Fremyella diplosiphon* cells. *Sensors (Basel)* **10**, 6969–6979.

Bordowitz, J. R., Whitaker, M. J. & Montgomery, B. L. (2010). Independence and interdependence of the photoregulation of pigmentation and development in *Fremyella diplosiphon*. *Commun Integr Biol* **3**, 151–153.

Campbell, D. (1996). Complementary chromatic adaptation alters photosynthetic strategies in the cyanobacterium *Calothrix*. *Microbiology* **142**, 1255–1263.

Castagna, A., Donnini, S. & Ranieri, A. (2009). Adaptation to iron-deficiency requires remodelling of plant metabolism: an insight in chloroplast biochemistry and functionality. In *Salinity and Water Stress*, pp. 205–212. Edited by M. Ashraf, M. Ozturk & H. R. Athar. Dordrecht: Springer.

Cobley, J. G., Zerweck, E., Reyes, R., Mody, A., Seludo-Unson, J. R., Jaeger, H., Weerasuriya, S. & Navankasattusas, S. (1993). Construction of shuttle plasmids which can be efficiently mobilized from *Escherichia coli* into the chromatically adapting cyanobacterium, *Fremyella diplosiphon*. *Plasmid* **30**, 90–105.

Connolly, E. L. & Guerinot, M. (2002). Iron stress in plants. *Genome Biol* **3**, S1024.

Dammeyer, T. & Frankenberg-Dinkel, N. (2008). Function and distribution of bilin biosynthesis enzymes in photosynthetic organisms. *Photochem Photobiol Sci* **7**, 1121–1130.

de Silva, D. M., Askwith, C. C. & Kaplan, J. (1996). Molecular mechanisms of iron uptake in eukaryotes. *Physiol Rev* **76**, 31–47.

Delcher, A. L., Bratke, K. A., Powers, E. C. & Salzberg, S. L. (2007). Identifying bacterial genes and endosymbiont DNA with Glimmer. *Bioinformatics* **23**, 673–679.

Ekman, M., Sandh, G., Nenninger, A., Oliveira, P. & Stensjö, K. (2014). Cellular and functional specificity among ferritin-like proteins in the multicellular cyanobacterium *Nostoc punctiforme*. *Environ Microbiol* **16**, 829–844.

Ferreira, F. & Straus, N. A. (1994). Iron deprivation in cyanobacteria. *J Appl Phycol* **6**, 199–210.

Fraser, J. M., Tulk, S. E., Jeans, J. A., Campbell, D. A., Bibby, T. S. & Cockshutt, A. M. (2013). Photophysiological and photosynthetic complex changes during iron starvation in *Synechocystis* sp. PCC 6803 and *Synechococcus elongatus* PCC 7942. *PLoS ONE* **8**, e59861.

Gutu, A. & Kehoe, D. M. (2012). Emerging perspectives on the mechanisms, regulation, and distribution of light color acclimation in cyanobacteria. *Mol Plant* **5**, 1–13.

Hantke, K. (2001). Iron and metal regulation in bacteria. *Curr Opin Microbiol* **4**, 172–177.

Hardie, L. P., Balkwill, D. L. & Stevens, S. E., Jr (1983a). Effects of iron starvation on the physiology of the cyanobacterium *Agmenellum quadruplicatum*. *Appl Environ Microbiol* **45**, 999–1006.

Hardie, L. P., Balkwill, D. L. & Stevens, S. E., Jr (1983b). Effects of iron starvation on the ultrastructure of the cyanobacterium *Agmenellum quadruplicatum*. *Appl Environ Microbiol* **45**, 1007–1017.

He, Y. Y. & Häder, D. P. (2002). Involvement of reactive oxygen species in the UV-B damage to the cyanobacterium *Anabaena* sp. *J Photochem Photobiol B* **66**, 73–80.

Kahn, K., Mazel, D., Houmard, J., Tandeau de Marsac, N. & Schaefer, M. R. (1997). A role for cpeYZ in cyanobacterial phycoerythrin biosynthesis. *J Bacteriol* **179**, 998–1006.

Kehoe, D. M. & Grossman, A. R. (1996). Similarity of a chromatic adaptation sensor to phytochrome and ethylene receptors. *Science* **273**, 1409–1412.

Kehoe, D. M. & Grossman, A. R. (1997). New classes of mutants in complementary chromatic adaptation provide evidence for a novel four-step phosphorelay system. *J Bacteriol* **179**, 3914–3921.

Kehoe, D. M. & Gutu, A. (2006). Responding to color: the regulation of complementary chromatic adaptation. *Annu Rev Plant Biol* **57**, 127–150.

Keren, N., Aurora, R. & Pakrasi, H. B. (2004). Critical roles of bacterioferritins in iron storage and proliferation of cyanobacteria. *Plant Physiol* **135**, 1666–1673.

Küpper, H., Setlík, I., Seibert, S., Prásil, O., Šetlikova, E., Strittmatter, M., Levitan, O., Lohscheider, J., Adamska, I. & Berman-Frank, I. (2008). Iron limitation in the marine cyanobacterium *Trichodesmium* reveals new insights into regulation of photosynthesis and nitrogen fixation. *New Phytol* **179**, 784–798.

Langmead, B., Trapnell, C., Pop, M. & Salzberg, S. L. (2009). Ultrafast and memory-efficient alignment of short DNA sequences to the human genome. *Genome Biol* **10**, R25.

Latifi, A., Jeanjean, R., Lemeille, S., Havaux, M. & Zhang, C.-C. (2005). Iron starvation leads to oxidative stress in *Anabaena* sp. strain PCC 7120. *J Bacteriol* **187**, 6596–6598.

Latifi, A., Ruiz, M. & Zhang, C. C. (2009). Oxidative stress in cyanobacteria. *FEMS Microbiol Rev* **33**, 258–278.

Lax, J. E., Arteni, A. A., Boekema, E. J., Pistorius, E. K., Michel, K. P. & Rögner, M. (2007). Structural response of photosystem 2 to iron deficiency: characterization of a new photosystem 2-IdiA complex from the cyanobacterium *Thermosynechococcus elongatus* BP-1. *Biochim Biophys Acta* **1767**, 528–534.

Lemasson, C., Marsac, N. T. & Cohen-Bazire, G. (1973). Role of allophycocyanin as light-harvesting pigment in cyanobacteria. *Proc Natl Acad Sci U S A* **70**, 3130–3133.

Michel, K. P. & Pistorius, E. K. (2004). Adaptation of the photosynthetic electron transport chain in cyanobacteria to iron deficiency: the function of IdiA and IsiA. *Physiol Plant* **120**, 36–50.

Montgomery, B. L. & Pattanaik, B. (2010). Regulation during adaptation of cyanobacteria to changes in iron availability: a case study of responses to iron limitation in *Fremyella diplosiphon*. In *Biometals: Molecular Structures, Binding Properties and Applications (Biotechnology in Agriculture, Industry and Medicine)*, pp. 215–226. Edited by G. Blanc & D. Moreau. Hauppauge, NY: Nova Science.

Narayan, O. P., Kumari, N. & Rai, L. C. (2011). Iron starvation-induced proteomic changes in *Anabaena* (*Nostoc*) sp. PCC 7120: exploring survival strategy. *J Microbiol Biotechnol* **21**, 136–146.

Pattanaik, B. & Montgomery, B. L. (2010). FdTonB is involved in the photoregulation of cellular morphology during complementary chromatic adaptation in *Fremyella diplosiphon*. *Microbiology* **156**, 731–741.

Rastogi, R. P., Singh, S. P., Häder, D.-P. & Sinha, R. P. (2010). Detection of reactive oxygen species (ROS) by the oxidant-sensing probe 2′,7′-dichlorodihydrofluorescein diacetate in the cyanobacterium *Anabaena variabilis* PCC 7937. *Biochem Biophys Res Commun* **397**, 603–607.

Regelsberger, G., Laaha, U., Dietmann, D., Rüker, F., Canini, A., Grilli-Caiola, M., Furtmüller, P. G., Jakopitsch, C., Peschek, G. A. & Obinger, C. (2004). The iron superoxide dismutase from the filamentous cyanobacterium *Nostoc* PCC 7120. Localization, overexpression, and biochemical characterization. *J Biol Chem* **279**, 44384–44393.

Sandström, S., Ivanov, A. G., Park, Y. I., Öquist, G. & Gustafsson, P. (2002). Iron stress responses in the cyanobacterium *Synechococcus* sp. PCC7942. *Physiol Plant* **116**, 255–263.

Shcolnick, S. & Keren, N. (2006). Metal homeostasis in cyanobacteria and chloroplasts. Balancing benefits and risks to the photosynthetic apparatus. *Plant Physiol* **141**, 805–810.

Sherman, D. M. & Sherman, L. A. (1983). Effect of iron deficiency and iron restoration on ultrastructure of *Anacystis nidulans*. *J Bacteriol* **156**, 393–401.

Singh, S. P. & Montgomery, B. L. (2011). Temporal responses of wild-type pigmentation and RcaE-deficient strains of *Fremyella diplosiphon* during light transitions. *Commun Integr Biol* **4**, 503–510.

Singh, S. P. & Montgomery, B. L. (2012). Reactive oxygen species are involved in the morphology-determining mechanism of *Fremyella diplosiphon* cells during complementary chromatic adaptation. *Microbiology* **158**, 2235–2245.

Singh, S. P. & Montgomery, B. L. (2013). Distinct salt-dependent effects impair *Fremyella diplosiphon* pigmentation and cellular shape. *Plant Signal Behav* **8**, e24713.

Sterner, R. W., Smutka, T. M., McKay, R. M. L., Xiaoming, Q., Brown, E. T. & Sherrell, R. M. (2004). Phosphorus and trace metal limitation of algae and bacteria in Lake Superior. *Limnol Oceanogr* **49**, 495–507.

Stowe-Evans, E. L., Ford, J. & Kehoe, D. M. (2004). Genomic DNA microarray analysis: identification of new genes regulated by light color in the cyanobacterium *Fremyella diplosiphon*. *J Bacteriol* **186**, 4338–4349.

Straus, N. A. (1994). Iron deprivation: physiology and gene regulation. In *The Molecular Biology of Cyanobacteria (Advances in Photosynthesis and Respiration)*, vol. 1, pp. 731–750. Edited by D. A. Bryant. Dordrecht: Kluwer.

Tandeau de Marsac, N. (1977). Occurrence and nature of chromatic adaptation in cyanobacteria. *J Bacteriol* **130**, 82–91.

Tandeau de Marsac, N. & Houmard, J. (1988). Complementary chromatic adaptation: physiological conditions and action spectra. *Methods Enzymol* **167**, 318–328.

Terry, M. J., Linley, P. J. & Kohchi, T. (2002). Making light of it: the role of plant haem oxygenases in phytochrome chromophore synthesis. *Biochem Soc Trans* **30**, 604–609.

Thompson, A. W., Huang, K., Saito, M. A. & Chisholm, S. W. (2011). Transcriptome response of high- and low-light-adapted *Prochlorococcus* strains to changing iron availability. *ISME J* **5**, 1580–1594.

Twiss, M. R., Auclair, J.-C. & Charlton, M. N. (2000). An investigation into iron-stimulated phytoplankton productivity in epipelagic Lake Erie during thermal stratification using trace metal clean techniques. *Can J Fish Aquat Sci* **57**, 86–95.

Walker, E. L. & Connolly, E. L. (2008). Time to pump iron: iron-deficiency-signaling mechanisms of higher plants. *Curr Opin Plant Biol* **11**, 530–535.

Xing, W., Huang, W. M., Li, D. H. & Liu, Y. D. (2007). Effects of iron on growth, pigment content, photosystem II efficiency, and siderophores production of *Microcystis aeruginosa* and *Microcystis wesenbergii*. *Curr Microbiol* **55**, 94–98.

Edited by: C.-C. Zhang